DOI: 10.1002/ejic.200800375

Crystal Structures and Magnetic Properties of 2D Supramolecular Architectures Assembled from Benzimidazolecarboxylato-Bridged 1D Double-Stranded Coordinating Chains Featuring Metallomacrocycles as Subunits

Shulan Ma,[a] Die Zhang,[a] Song Gao,[b] Yong He,[a] Hui Ma,[c] Chuanmin Qi,*[a] Cuihong Fan,[a] Yufeng Chen,[a,d] and Xiaojing Yang[a]

Keywords: Manganese(II) complexes / Benzimidazolecarboxylic acid / Double-stranded coordinating chain / Metallomacrocycles / Magnetic properties

Two new 2D supramolecular architectures $[\{Mn_2(L_1)_2(H_2O)_2\}\cdot 2CH_3OH]_n$ (**1**) and $[\{Mn_2(L_2)_2(CH_3OH)_4\}\cdot 2CH_3OH\cdot 4(H_2O)]_n$ (**2**) were assembled from the newly synthesised semi-rigid ligands H_2L_1 {2,6-bis[(6-carboxy-2,4-dimethylbenzimidazol-1-yl)methyl]pyridine} and H_2L_2 {2,6-bis[(6-carboxy-4-methyl-2-propylbenzimidazol-1-yl)methyl]pyridine} by reaction with Mn^{II} ions. They both contain novel 1D double-stranded coordinating chains with metallomacrocyclic subunits and dinuclear Mn^{II} subrings bridged by benzimidazolecarboxylato ions, the latter derived from the ligands. The differences in the steric hindrance of the methyl and propyl groups attached to the benzimidazole rings in H_2L_1 and H_2L_2 led to different coordinating modes of the carboxylato groups and, thus, aesthetically fascinating extended structures with useful magnetic properties. Variable-temperature susceptibility measurements (2–300 K) revealed antiferromagnetic coupling interactions (J = –0.23 cm^{-1} for **1** and –0.92 cm^{-1} for **2**) with values being within the reported range but differing from each other due to the distinct bridging modes of the carboxylato ions. The different crystal structures and magnetic properties of **1** and **2** are discussed in detail.

(© Wiley-VCH Verlag GmbH & Co. KGaA, 69451 Weinheim, Germany, 2008)

Introduction

Currently, there is great interest in metal-organic hybrid materials containing paramagnetic metal ions within extended structures. This is driven, to a large extent, by their fascinating network topologies and potential application in the field of molecular magnetism.[1] The low-dimensional (1D chain-like or 2D layer-like) extended structures have attracted special interest on account of their specific structural features and unusual nonlinear optical and magnetic properties.[2] Therefore, rational design and construction of new materials with specific network structures and subsequent investigation of their properties have become particularly important and topical subjects. One commonly used strategy for constructing such extended networks is to select appropriate bridging ligands which can transmit magnetic interactions in addition to binding several metal ions in specific coordination geometries. The type, size, shape, flexibility, conformation and symmetry of the ligands along with their connective patterns are all important parameters, affecting the type and magnitude of the magnetic exchange interactions.[3] In the course of the formation of complexes with desirable magnetic properties, certain features of the organic ligands connecting paramagnetic metal centres can be utilised and tuned. Accordingly, polycarboxylic ligands are good candidates for this purpose. The carboxyl group can not only bridge two or more metal centres to produce a wide variety of complexes ranging from zero-dimensional discrete molecules to 3D architectures but also adopt various bridging conformation modes. The magnetic properties of the complexes are closely dependent on the bridging modes adopted by the carboxyl groups.[4]

It is known that high-spin manganese(II) contains five unpaired electrons, is quite oxophilic and that the assembly of manganese(II) with organic ligands containing the carboxyl group is inclined to the formation of larger clusters and extended solids.[5] Moreover, the (carboxylato)manganese(II) complexes have long been of special interest since they are known to exist at the active sites of some Mn^{II}-containing metalloenzymes.[6]

In addition, metallomacrocycles being prepared from an increasing variety of metals and organic ligands have become of particular interest recently for having internal cavities which can accommodate other molecules for such di-

[a] College of Chemistry, Beijing Normal University, Beijing 100875, China
Fax: +86-10-58802075
E-mail: qicmin@sohu.com
mashulan@bnu.edu.cn
[b] State Key Laboratory of Rare Earth Materials Chemistry and Applications, College of Chemistry and Molecular Engineering, Peking University, Beijing 100871, China
[c] Analytical and Testing Centre, Beijing Normal University, Beijing 100875, China
[d] Department of Chemistry, Nanchang University, Nanchang 330031, China

 WILEY InterScience DISCOVER SOMETHING GREAT © 2008 Wiley-VCH Verlag GmbH & Co. KGaA, Weinheim

verse applications as gas storage, selective inclusion and separation.[7] The metal-driven self-assembly of macrocycles is currently considered as a powerful tool for designing various metallomacrocycles of different shapes and geometries[8] which are often obtained in one step and in higher yields than those obtained by more tedious classical organic methods.[9] Their preparation can be easily achieved by using metal ions which directionally form dative bonds with the bridging ligands, providing the ultimate metallomacrocycle with different shapes.[10]

Owing to the presence of many subtle factors in the assembly process and the difficulty in predicting the final architectures, the rational design of functional supramolecular complexes from organic ligands and metal ions is still a challenge to chemists, and a great deal of work is required to extend the knowledge of relevant magnetic solids and establish proper synthetic strategies leading to desirable architectures and useful properties. Hence, we newly prepared two benzimidazolecarboxylic acid ligands H_2L_1 {2,6-bis[(6-carboxy-2,4-dimethylbenzimidazol-1-yl)methyl]-pyridine} and H_2L_2 {2,6-bis[(6-carboxy-4-methyl-2-propylbenzimidazol-1-yl)methyl]pyridine} from which two Mn^{II} polymers $[\{Mn_2(L_1)_2(H_2O)_2\}\cdot 2CH_3OH]_n$ (**1**) and $[\{Mn_2(L_2)_2(CH_3OH)_4\}\cdot 2CH_3OH\cdot 4(H_2O)]_n$ (**2**) could be obtained separately after treatment with $Mn(AcO)_2$. They both exhibit 2D supramolecular architectures assembled from double-stranded chains containing a novel metallomacrocycle and a less common dinuclear subring, of which the latter induces the useful magnetic coupling. We report, herein, the crystal structures and magnetic properties of **1** and **2**.

Results and Discussion

The Syntheses of the Ligands and Complexes

From a structural point of view of benzimidazole (Bim) derivatives such as benzimidazolecarboxylic acid, the deprotonated ligand possesses two interesting characteristics: (1) the N atoms in the Bim ring and the O atoms in carboxylato group are both potential sites for hydrogen-bonding interactions, given that solvent molecules such as water or methanol serve as possible hydrogen-bonding donors; (2) resulting from the Bim rings, π–π interactions might contribute greatly to the formation of the observed crystal structures and enhance the stability of the resultant supramolecular architectures.[11]

Su et al. have synthesised semi-rigid bi-/tridentate ligands constructed around central arene groups and extended with Bim arms, and prepared model complexes with well-defined trigonal or tetragonal prismatic shapes by using these ligands.[12] They also prepared a series of dinuclear rectangular-shaped macrocycles as well as trigonal- or tetragonal-prismatic 3D cages by using those ligands.[13] All these show that the semi-rigid angular ditopic ligands are good candidates for the construction of various metallomacrocycles. For our present ligands, two Bim rings are connected by means of methylene groups in the 1-positions of the pyridine rings to create semi-rigid compounds with two arms that can rotate freely around C–C bonds. Compared with those compounds mentioned above,[12,13] two additional carboxylato arms in H_2L_1 and H_2L_2 may increase the flexibility, thereby promoting the metallomacrocycles. The bridging function of the carboxylato groups can induce the formation of the dinuclear Mn^{II} subunit and finally the 1D double-stranded chains of complexes **1** and **2**, the structures of which differ significantly from the before-mentioned complexes.[12,13] Additionally, the much longer distance of the carboxylato groups in H_2L_1 and H_2L_2 may inhibit the expansion of polymeric frameworks enabling the formation of the desired low-dimensional structures.

Complexes **1** and **2** were initially synthesised by conventional solution reactions of ligands H_2L_1 and H_2L_2 with $Mn(AcO)_2$ under room temperature conditions with an Mn/ligand molar ratio of 1:1. In order to investigate the influence of the solvent on the growth of the crystals, the reactions were carried out under similar evaporating conditions and the same pH value of 7 with different solvents. The $CH_2Cl_2/CH_3OH/Et_3N$ mixed solvent evaporated too quickly to give crystals. In the $CH_3OH/CH_3CN/H_2O$ solvent system with NaOH solution (adjusting the pH value), the complexes are always formed in clusters. By using a CH_3OH/H_2O solvent with NaOH solution, we found that single crystals grew much more easily with good shapes and sizes suitable for X-ray analysis (CH_3OH/H_2O ratio of 3:1 and 6:1 for **1** and **2**, respectively). Crystals of **1** and **2** are preferably obtained from reactions of the ligands with $Mn(AcO)_2$. When replacing $Mn(AcO)_2$ with other manganese salts such as $MnCl_2$, single crystals of **1** and **2** cannot be easily obtained. The hydrothermal method is routinely adopted in the synthesis of carboxylato complexes but, it is not a good method for **1** and **2**. We found that hydrothermal reactions always give powders or poorly defined crystal-like products but not single crystals. From IR spectroscopy and element analysis, the poorly defined crystal-like product was the same phase as our product. However, because of the poor solubilities of the ligands, the powder samples were mixtures of the reactants and the resultant complexes.

IR Spectroscopy

The IR spectra of **1** and **2** offer some valuable information about the metal–ligand bonding and the coordination modes of the carboxylato groups. The strong absorptions at 1683 and 1676 cm^{-1} for H_2L_1 and H_2L_2 were assigned to the ν(C=O) stretching vibration of the carboxylic groups. The frequencies of these vibrations are slightly lower than those of the nonassociated carboxylic C=O groups, supporting the conclusion that the carboxylic groups may participate in intermolecular hydrogen bonding. The absence of any strong absorptions around 1700 cm^{-1} expected for the vibrations of protonated carboxyl groups (–COOH) in **1** and **2** indicates that all carboxyl groups are deprotonated, and the significant shifts to lower wave numbers of the bands of the carboxylic groups

 © 2008 Wiley-VCH Verlag GmbH & Co. KGaA, Weinheim

indicate the coordination of the carboxylato oxygen atoms to the metal ions. The very strong absorption bands at 1271 and 1239 cm^{-1} in H_2L_1 (1277 cm^{-1} in H_2L_2) assigned to the C–O stretching vibrations[14] are all absent in complexes **1** and **2**, also indicating the deprotonation and coordination of the carboxylic groups. Amongst the four strong absorptions at 1549, 1537, 1418 and 1395 cm^{-1} for **1** (1576, 1542, 1416 and 1399 cm^{-1} for **2**), the bands at 1549 and 1537 cm^{-1} for **1** (1576 and 1542 cm^{-1} for **2**) can be attributed to ν_{as}(–COO^-). The splitting of the ν_{as}(–COO^-) band indicates that both carboxylato groups are in different coordination modes,[15] and this is consistent with their respective crystal structures. The bands at 1418 and 1395 cm^{-1} in **1** may correspond to the ν_s(–COO^-) band of the bidentate chelating and chelating-bridging tridentate carboxylato groups, respectively, whereas those at 1416 and 1399 cm^{-1} in **2** may correspond to ν_s(–COO^-) bands of the chelating bidentate and bridging bidentate carboxylato groups, respectively.[16]

Description of the Crystal Structures

Complexes **1** and **2** both consist of 1D double-stranded chains. Two neighbouring Mn^{II} ions are wrapped by four ligands giving a dinuclear subring. Meanwhile, four Mn^{II} atoms are bridged by carboxylato groups from two ligands producing a metallomacrocycle. Selected bond lengths and angles of **1** and **2** are summarised in Tables 1 and 2, respectively.

Crystal Structure of Complex 1

As shown in Figure 1, the Mn1 ion in **1** is coordinated to six oxygen atoms, two (O2, O3) from one chelating bi-

Table 1. Selected bond lengths [Å] and bond angles [°] for **1**.

Bond lengths			
Mn(1)–O(1)	2.096(2)	Mn(1)–O(2)	2.235(2)
Mn(1)–O(3)	2.240(3)	Mn(1)–O(5)#2	2.142(2)
Mn(1)–O(4)#3	2.275(2)	Mn(1)–O(5)#3	2.302(2)
O(4)–Mn(1)#1	2.275(2)	O(5)–Mn(1)#1	2.302(2)
O(5)–Mn(1)#2	2.142(2)	C(1)–O(2)	1.253(4)
C(1)–O(3)	1.261(4)	C(27)–O(4)	1.253(4)
C(27)–O(5)	1.275(4)	C(9)–N(1)	1.329(4)
C(9)–N(2)	1.363(4)	C(18)–N(4)	1.362(4)
C(18)–N(5)	1.318(4)		
Bond angles			
O(1)–Mn(1)–O(2)	89.87(9)	O(1)–Mn(1)–O(3)	139.12(10)
O(1)–Mn(1)–O(5)#2	104.77(9)	O(1)–Mn(1)–O(4)#3	96.93(9)
O(1)–Mn(1)–O(5)#3	102.67(9)	O(2)–Mn(1)–O(3)	58.52(9)
O(2)–Mn(1)–O(4)#3	122.81(9)	O(2)–Mn(1)–O(5)#3	167.44(9)
O(3)–Mn(1)–O(4)#3	82.31(9)	O(3)–Mn(1)–O(5)#3	110.43(9)
O(4)#3-Mn(1)–O(5)#3	56.86(8)	O(5)#2-Mn(1)–O(2)	101.38(9)
O(5)#2-Mn(1)–O(3)	106.36(10)	O(5)#2-Mn(1)–O(4)#3	130.56(8)
O(5)#2-Mn(1)–O(5)#3	75.10(8)	Mn(1)#2-O(5)–Mn(1)#1	104.90(8)
C(27)–O(4)–Mn(1)#1	92.57(18)	C(27)–O(5)–Mn(1)#2	157.0(2)
C(27)–O(5)–Mn(1)#1	90.75(18)		

Symmetry transformations used to generate equivalent atoms: #1: $x + 1, y - 1, z - 1$; #2: $-x + 1, -y + 2, -z$; #3: $x + 1, y - 1, z - 1$.

Table 2. Selected bond lengths [Å] and bond angles [°] for **2**.

Bond lengths			
Mn(1)–O(1)	2.079(3)	Mn(1)–O(2)#1	2.061(4)
Mn(1)–O(3)#2	2.350(4)	Mn(1)–O(4)#2	2.210(4)
Mn(1)–O(5)	2.238(4)	Mn(1)–O(6)	2.214(4)
C(18)–O(1)	1.248(6)	C(18)–O(2)	1.257(6)
C(31)–O(3)	1.262(6)	C(31)–O(4)	1.258(6)
C(7)–N(2)	1.365(6)	C(7)–N(3)	1.324(6)
C(20)–N(4)	1.367(6)	C(20)–N(5)	1.310(7)
Bond angles			
O(1)–Mn(1)–O(2)#1	108.70(15)	O(1)–Mn(1)–O(3)#2	93.85(14)
O(1)–Mn(1)–O(4)#2	150.89(15)	O(1)–Mn(1)–O(5)	91.55(17)
O(1)–Mn(1)–O(6)	92.12(18)	O(2)#1-Mn(1)–O(3)#2	157.36(14)
O(2)#1-Mn(1)–O(4)#2	100.19(15)	O(2)#1-Mn(1)–O(5)	93.13(17)
O(2)#1-Mn(1)–O(6)	91.31(17)	O(4)#2-Mn(1)–O(5)	83.19(16)
O(4)#2-Mn(1)–O(6)	90.73(17)	O(4)#2-Mn(1)–O(3)#2	57.49(13)
O(5)–Mn(1)–O(3)#2	88.13(14)	O(6)–Mn(1)–O(3)#2	85.71(15)
O(6)–Mn(1)–O(5)	173.02(16)		

Symmetry transformations used to generate equivalent atoms: #1 $-x + 2, -y + 3, -z + 1$; #2: $x, y + 1, z + 1$; #3: $x, y - 1, z - 1$.

 © 2008 Wiley-VCH Verlag GmbH & Co. KGaA, Weinheim

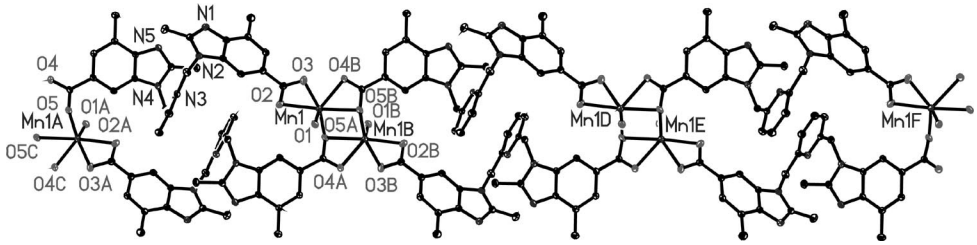

Figure 1. View of the 1D coordinating chains containing the metallomacrocycles and dinuclear subrings in **1**.

dentate carboxylato group from one ligand, three [O5A (–*x* + 1, –*y* + 2, –*z*), O4B and O5B (*x* + 1, *y* – 1, *z* – 1)] from two chelating-bridging tridentate carboxylato groups from two ligands and one (O1) from one water molecule, giving a distorted octahedral geometry. The O2, O4B, O5A and O5B centres constitute the basal plane (mean deviation 0.0287 Å) and O1 and O3 occupy the axial positions with the Mn1 ion being displaced by 0.2742 Å out of this plane towards O1. The most distorted angle of the octahedron may be due to the bite angle of the tridentate carboxylato groups [O4B–Mn(1)–O5B, 56.86°]. The carboxylato group can adopt various conformation modes such as monodentate, chelating/bridging-bidentate (*syn-syn*, *syn-anti* and *anti-anti*) and multidentate (Scheme 1). They may, therefore, function as bridging ligands to form multinuclear coordination polymers, thus bringing about novel topologies and versatile magnetic properties. One carboxylato group (C1/O2/O3) of the ligand exhibits a chelating bidentate mode, whereas another (C27/O4/O5) shows the chelating-bridging tridentate mode. For the tridentate C27/O4/O5, the bidentate C27–O5 bond (1.275 Å) is more elongated than the monodentate C27–O4 (1.253 Å), while for C1/O2/O3 with an equivalent mode, the value of the C1–O2 bond (1.253 Å) is close to that of C1–O3 (1.261 Å). Meanwhile, C27/O4/O5 is more twisted to its attached Bim ring N4/N5/C18–C25 with an angle of 22.4°, whereas C1/O2/O3 has a smaller twist to its Bim ring N1/N2/C2–C9 with an angle of 12.1°. The greater twist in the former may be due to the asymmetrical mode and the subsequent π interaction concerning N4/N5/C18–C25. Whatever the case, the C–O bonds in two carboxylato groups are relatively symmetric, indicating the delocalisation and deprotonation of the carboxylato groups. In the dinuclear subring, the Mn–Mn distance [Mn1–Mn1B (–*x* + 2, –*y* + 1, –*z* – 1)] is 3.525 Å. The dihedral angle of 93.1° (89.2°) between the Bim planes N1/N2/C2–C9 (N4/N5/C18–C25) and the pyridine ring N3/C12–C16 shows that two Bim planes are nearly perpendicular to the pyridine core.

There are π–π interactions between the Bim rings N4/N5/C18–C25 and N4AC/N5AC/C18AC–C25AC (–*x* + 1, –*y* + 2, –*z* + 1) in neighbouring chains with a plane-to-plane distance of 3.450 Å. According to Janiak's report, these belong to the stronger π-stacking interactions.[11] There are hydrogen bonds N1···H2#1–O1#1 (*x*, *y*, *z* + 1) (N1···O1#1, 2.846 Å) and N5···H1#1–O1#1 (N5···O1#1, 2.704 Å) between the Bim nitrogen atoms and the coordinated oxygen atoms of the water molecules. (In the description of hydrogen bonds, for clarity, the atoms generated by symmetry operations are indicated by "#*n*", where *n* is an integer.) All these π-interactions and hydrogen bonds join

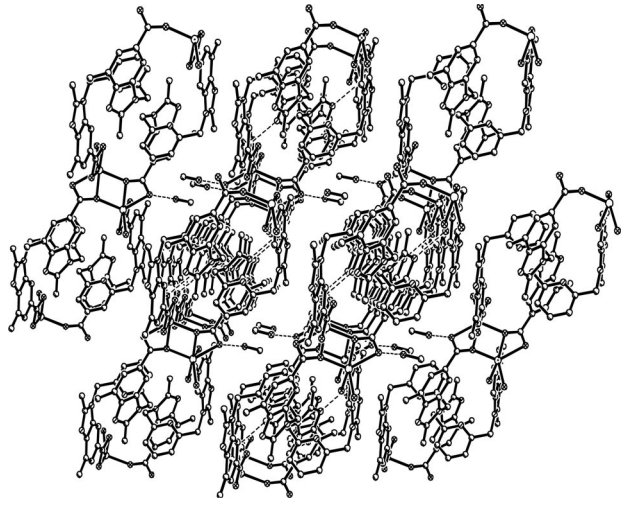

Figure 2. Channels between 2D networks in **1** viewed along the *c*-axis. Hydrogen bonds are shown as dashed lines.

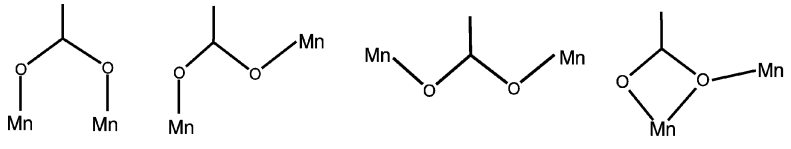

Scheme 1. Schematic representations of the coordination modes of the carboxylato bridges.

 © 2008 Wiley-VCH Verlag GmbH & Co. KGaA, Weinheim

the chains forming 2D supramolecular networks. The nearest intrachain Mn–Mn distance (14.990 Å) among the metallomacrocycles except in the dinuclear subrings is longer than the nearest interchain Mn–Mn distance (8.391 Å). This situation resembles other reported 1D double-stranded chained complexes.[17] There exist channels between the networks which accommodate solvated methanol molecules. The methanol molecules form the hydrogen bond O4···H6#2–O6#2 ($-x$, $-y + 2$, $-z + 1$) (O4···O6#2, 2.852 Å) with a coordinated carboxylato group (Figure 2).

Crystal Structure of Complex 2

The Mn1 ion in **2** is six-coordinated by O1 and O2A ($-x + 2$, $-y + 3$, $-z + 1$) from two bridging bidentate carboxylato groups, O3B and O4B (x, $y + 1$, $z + 1$) from one chelating bidentate carboxylato group, and O5 and O6 from methanol molecules (Figure 3) giving a more regular octahedral geometry than observed in **1**. Atoms O1, O2A, O3B and O4B make up the basal plane (mean deviation is 0.0649 Å), whereas O5 and O6 occupy the axial positions, with the Mn1 ion being displaced by 0.0121 Å from of this plane towards O6. The most distorted angle of the octahedron may be due to the bite angle of the chelating carboxylato groups (O3B–Mn1–O4B, 57.49°). Two carboxylato groups in the dinuclear subring adopt a *syn-syn* bridging arrangement binding two Mn ions with an Mn–Mn distance [Mn1–Mn1A ($x + 1$, $y - 1$, $z - 1$)] of 4.473 Å which is longer than in **1**. One carboxylato group (C18/O1/O2) shows the bridging bidentate mode, while another (C31/O3/O4) exhibits the chelating bidentate mode, a situation different from that observed in **1**. The two carboxylato ions are both nearly coplanar (14.7° and 14.2°), and their own attached Bim rings show a smaller twist due to the smaller differences in the C–O coordination modes. The closer C–O distances (1.248 and 1.257 Å for C18/O1/O2, 1.262 and 1.258 Å for C31/O3/O4) are also due to the symmetric coordination modes. The dihedral angles of the Bim planes N2/N3/C7/C11–C16 with the pyridine ring N1/C1–C5 and N4/N5/C20/C24–C29 with N1/C1–C5 are 84.4° and 79.6°, respectively.

There also exist π-interactions in **2** between the Bim rings N4/N5/C20/C24–C29 and N4E/N5E/C20E/C24E–C29E ($-x + 2$, $-y + 1$, $-z$) with a plane-to-plane distance of 3.508 Å and hydrogen bonds between the Bim nitrogen atoms and oxygen atoms of the water and methanol molecules [N5···O5#3 ($-x + 2$, $-y + 2$, $-z + 1$) 2.848 Å, N3···O8

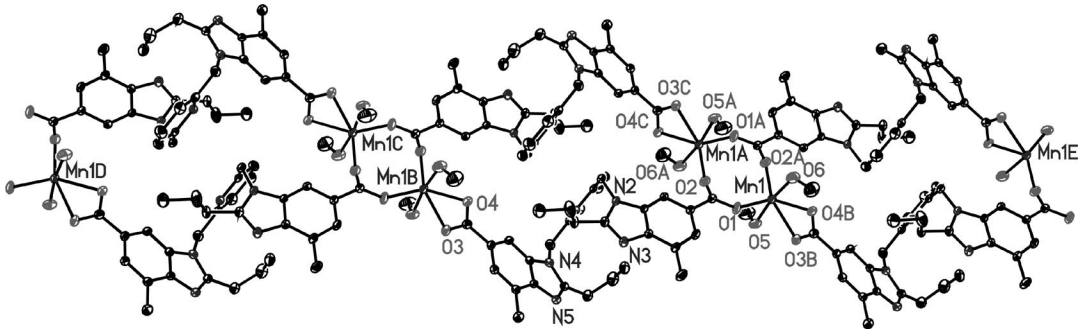

Figure 3. View of the 1D coordinating chains containing metallomacrocycles in **2**.

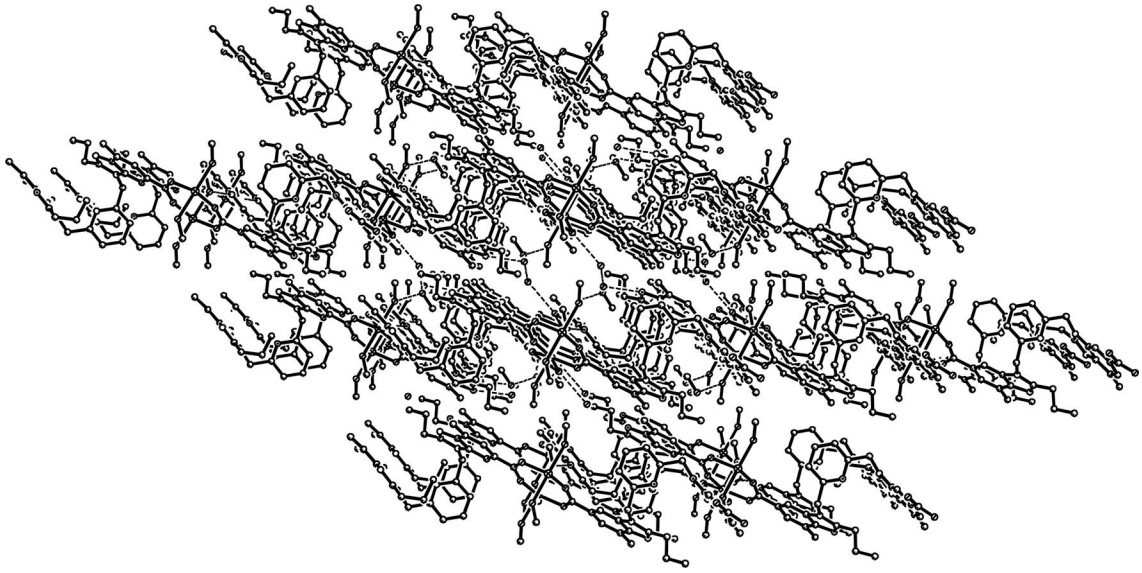

Figure 4. Channels in the supramolecular network of **2** viewed along the *c*-axis. Hydrogen bonds are shown as dashed lines.

 © 2008 Wiley-VCH Verlag GmbH & Co. KGaA, Weinheim

2.867 Å, O8···O9 2.821 Å, O9···O7 2.703 Å, O7···O6#4 (x, $y-1$, z) 2.638 Å] in two adjacent chains. All the π–π interactions and hydrogen bonds link the 1D chains into 2D networks. The channels, in the supramolecular network, which accommodate solvated molecules, are shown in Figure 4. The nearest intrachain M–M distance (13.945 Å) in the metallomacrocycle in **2** is longer than the interchain Mn–Mn distance (7.798 Å). Compared with other reported double-stranded chain complexes,[16,18] the intrachain M–M distances in **1** and **2** are much longer, possibly due to the greater length of our ligands.

Magnetic Properties

The variable-temperature magnetic susceptibilities of **1** and **2** were measured in the range of 2.0–300 K at 1000 Oe as shown in Figure 5. The $\chi_m T$ values at room temperature are 8.52 and 8.56 $cm^3 mol^{-1} K$ for **1** and **2**, respectively, which are close to the expected value of 8.75 $cm^3 mol^{-1} K$ for two independent spins $S = 5/2$. Upon cooling from room temperature, the $\chi_m T$ values for **1** and **2** both decrease smoothly at first until 50 K and then sharply at lower temperature reaching values of 4.94 (for **1**) and 1.37 $cm^3 mol^{-1} K$ (for **2**) at 2.0 K. The χ_m^{-1} vs. T plots are essentially linear for **1** and **2**, and least-squares fitting of the data to the Curie–Weiss law gave $C = 8.52$ $cm^3 mol^{-1} K$ and $\theta = -1.26$ K for **1**, and $C = 8.72$ $cm^3 mol^{-1} K$ and $\theta = -5.27$ K for **2**. The decreases in the $\chi_m T$ values upon cooling and the negative Weiss constants indicate that there exist antiferromagnetic interactions between Mn^{II} centres. It is worth noting the quite different $\chi_m T$ scales of 4.94–8.52 $cm^3 mol^{-1} K$ for **1** and 1.37–8.56 $cm^3 mol^{-1} K$ for **2**. This feature corresponds to the different magnetic behaviour of **1** and **2**, indicating the stronger antiferromagnetic coupling in **2**.

Considering the long intrachain Mn–Mn separations in the metallomacrocycles (14.990 and 13.945 Å for **1** and **2**, respectively) and the long interchain Mn–Mn distances (8.391 and 7.798 Å for **1** and **2**, respectively), the magnetic interactions between Mn^{II} ions except in the dinuclear subrings seem negligible. The magnetic data of **1** and **2** were therefore analysed as a dinuclear system and fitted through Equation (1) for dimers.[19]

$$\chi_M = \frac{2Ng^2\beta^2}{kT} \times \frac{55+30\exp(5x)+14\exp(9x)+5\exp(12x)+\exp(14x)}{11+9\exp(5x)+7\exp(9x)+5\exp(12x)+3\exp(14x)+\exp(15x)}$$

$$\text{with} \quad x = -J/kT \tag{1}$$

The experimental data fit well and lead to $g = 1.97$, $J = -0.23$ cm^{-1} and $R = 2.65 \times 10^{-5}$ for **1**, and $g = 2.00$, $J = -0.92$ cm^{-1}, $R = 1.10 \times 10^{-4}$ for **2** ($R = \Sigma[\chi_m T_{obs} - \chi_m T_{calc}]^2 / \Sigma[\chi_m T_{obs}]^2$). The solid lines in Figures 5a and b represent the best fit of the experimental data.

The J values, reported in the literature, for materials with only carboxylato groups as bridging ligands are usually small and negative, between approximately –0.2 and –5.0 cm^{-1}, indicating weak antiferromagnetic coupling.[20] The J values of **1** and **2** are well within the reported range but differ from each other which maybe due to the distinct coordination modes of the carboxylato ions. In **1**, two carboxylato groups bridge two Mn^{II} ions in a chelating-bridging tridentate fashion (Scheme 1d), providing a novel interaction pathway, whereas in **2**, two carboxylato ions bridge two Mn^{II} ions in a *syn-syn* bidentate fashion (Scheme 1a).

The magnetic exchange coupling found for carboxylato-bridged complexes is largely determined by the bridging conformation[21] and the interaction between the d orbitals of the metal ion and the bridge. The magnitude of the antiferromagnetic interaction depends on the overlap of the magnetic orbitals centred on the nearest-neighbour metal ions. The *syn-syn* mode provides small metal–metal distances and a good overlap of magnetic orbitals which usually induces antiferromagnetic coupling in Mn^{II} polynuclear complexes.[22] The *syn-anti* mode induces much smaller J values, because two metal centres are considerably ex-

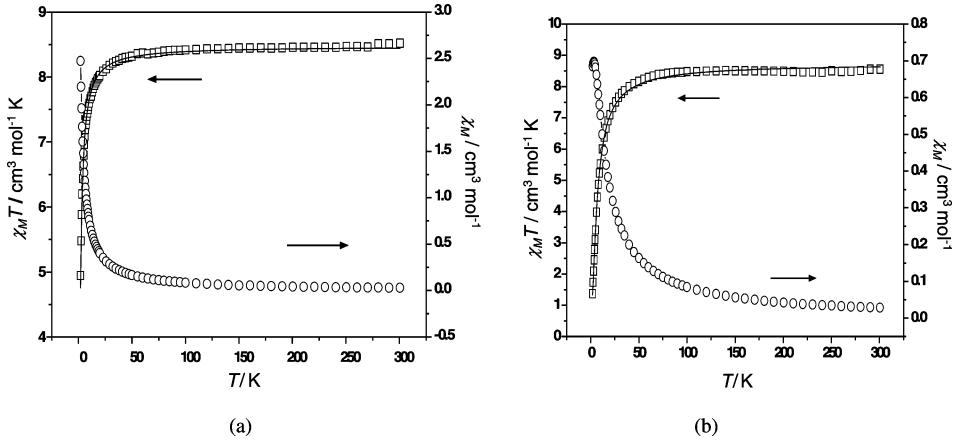

Figure 5. Plots of the temperature dependence of χ_m (circles) and $\chi_m T$ (squares) of **1** (a) and **2** (b) measured at 1000 Oe. The solid lines represent the best fit of the experimental data as discussed in the text.

 © 2008 Wiley-VCH Verlag GmbH & Co. KGaA, Weinheim

panded and the 2p orbitals of O and O′ belonging to the magnetic orbitals centred on M and M′, respectively, are unfavourably oriented to give a strong overlap, thus causing a reduction of the antiferromagnetic contribution, maybe leading ultimately to overall ferromagnetic behaviour.[4a,23] The few examples involving the *anti-anti* mode indicate that the coupling is weakly ferromagnetic or antiferromagnetic.[4a,24]

The effect of the far less common chelating-bridging tridentate mode of carboxyl groups in **1** may be looked on as a combination of the *syn-anti* configuration and the μ-O bridges.[25] DFT calculations on Mn–O–Mn systems indicate a stronger antiferromagnetic coupling when the Mn–O–Mn angle is below 98° and a weak antiferromagnetic response for angles in the ca. 98–110° range.[26] The Mn1–O5A–Mn1B angle of 104.9° in **1** is in the 98–110° range, so the weak antiferromagnetic coupling J (–0.23 cm^{-1}) is understandable. Thus, the *syn-anti* conformation and the Mn–O–Mn angle of 104.9° lead to the overall reduction of the antiferromagnetic interaction and the smaller magnitude.

Conclusions

Two new 2D supramolecular architectures can be assembled from novel 1D double-stranded coordinating chains with metallomacrocyclic subunits and a dinuclear subring bridged by benzimidazolecarboxylato ions. Their structural particularities indicate that only differences in the steric effects of the propyl and methyl groups attached to the Bim rings play an important role in tuning the topologies which further influence the magnetic properties. The chelating-bridging tridentate mode of the carboxylato ion in **1** provides a less common interaction pathway which may reduce the antiferromagnetic contribution but lead to promising ferromagnetic behaviour. We are currently extending the synthetic studies of these kinds of ligands but with a smaller steric hindrance of the central groups so as to produce larger internal cavities in the metallomacrocycles and complexes with other metal ions. We also plan to investigate their other properties, in particular inclusion chemistry, fluorescence behaviour and further supramolecular assemblies.

Experimental Section

General: 3-methyl-4-nitrobenzenecarboxylic acid and other commercially available chemicals were of analytical grade and were used without further purification. Methyl 2,7-dimethyl-3*H*-benzoimidazole-5-carboxylate (A_1) and methyl 7-methyl-2-propyl-3*H*-benzoimidazole-5-carboxylate (B_1) were synthesised from 3-methyl-4-nitrobenzenecarboxylic acid according a reported procedure.[27] The preparation of 2,6-bis(bromomethyl)pyridine was carried out according to the literature.[28] C, H and N compositions were determined by using an Elementar Vario EL elemental analyser. UV/Vis spectra were measured, in MeOH solution, by using a GBC Cintra 10e UV/Vis spectrophotometer. IR spectra were recorded with a Nicolet-AVATAR 360 FTIR spectrometer by using KBr pellets in the 4000–400 cm^{-1} region. NMR spectra were recorded with a Varian 500 Bruker spectrometer in [D_6]DMSO or $CDCl_3$. Variable-temperature magnetic susceptibility data for the crystalline samples of complexes **1** and **2** were recorded in an external field of 1000 G with an Oxford Maglab 2000 system magnetometer in the 2–300 K temperature range. The susceptibilities were corrected for diamagnetism with Pascal's constants for all the constituent atoms, and magnetic moments were calculated by using the equation $\mu_{eff} = 2.828 (\chi_m T)^{1/2}$.

Syntheses and Characterisation: The ligands H_2L_1 and H_2L_2 and their precursors were prepared according to Scheme 2.

Synthesis of A_2: To a CH_3CN solution (30 mL) of A_1 (0.408 g, 2.0 mmol) at 0 °C was added NaH (0.192 g, 8.0 mmol). The mixture was stirred at room temperature for 1 h and 2,6-bis(bromomethyl)pyridine (0.264 g, 1.0 mmol) was then added and stirring continued for 6 h. The solvent was removed under reduced pressure to give a white solid which was purified by column chromatography (silica gel; ethyl acetate/methanol, 20:1) to afford the product A_2. Yield: 0.222 g, 45.87%. M.p. 238–241 °C. ^{1}H NMR (500 MHz, $CDCl_3$): δ = 7.86 (s, 2 H, Ar-H), 7.81 (s, 2 H, Ar-H), 7.53 (t, J = 7.6 Hz, 1 H, pyridine-H), 6.78 (d, J = 7.6 Hz, 2 H, pyridine-H), 5.43 (s, 4 H, pyridine-CH_2), 3.93 (s, 6 H, OCH_3), 2.72 (s, 6 H, N=CCH_3), 2.63 (s, 6 H, Ar-CH_3) ppm. ^{13}C NMR ([D_6]DMSO, 125 MHz): δ = 167.29, 156.17, 155.48, 145.68, 138.84, 134.90, 128.15, 123.07, 122.98, 121.29, 109.79, 52.30, 48.27, 16.74, 14.04 ppm. IR (KBr pellet): $\tilde{\nu}$ = 3554, 3367, 3280, 2950, 1725, 1692, 1595, 1515, 1438, 1417, 1381, 1351, 1287, 1244, 1222, 1201, 1182, 1070, 991, 884, 798, 773, 611 cm^{-1}.

Synthesis of B_2: To a CH_3CN solution (30 mL) of B_1 (0.464 g, 2.0 mmol) at 0 °C was added NaH (0.192 g, 8.0 mmol). The mixture was stirred at room temperature for 1 h and 2,6-bis(bromomethyl)pyridine (0.264 g, 1.0 mmol) was then added and stirring continued for 6 h. The solvent was removed under reduced pressure to give a white solid which was purified by column chromatography (silica gel; petroleum ether/ethyl acetate, 2:1) to afford B_2. Yield:

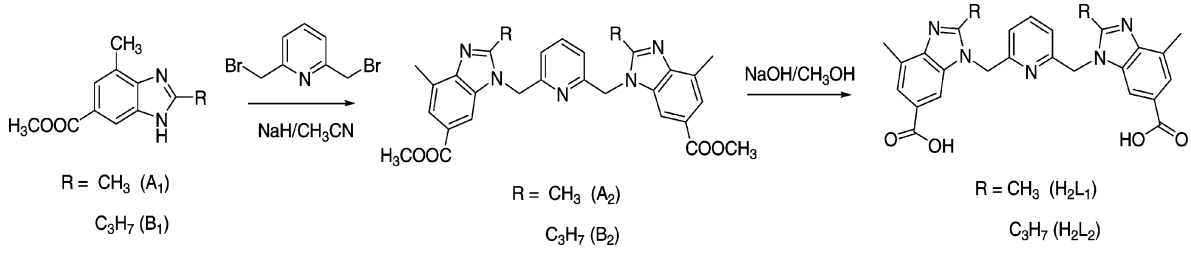

Scheme 2. Synthetic routes for the ligands H_2L_1 and H_2L_2.

 © 2008 Wiley-VCH Verlag GmbH & Co. KGaA, Weinheim

0.35 g, 68.12%. M.p. 247–249 °C. ^{1}H NMR (500 MHz, $CDCl_3$): δ = 7.84 (s, 2 H, Ar-H), 7.80 (s, 2 H, Ar-H), 7.49 (t, J = 7.79 Hz, 1 H, pyridine-H), 6.70 (d, J = 7.79 Hz, 2 H, pyridine-H), 5.46 (s, 4 H, pyridine-CH_2), 3.92 (s, 6 H, OCH_3), 2.85 (t, J = 7.75 Hz, 4 H,$CH_2C_2H_5$), 2.74 (s, 6 H, Ar-CH_3), 1.82 (m, 4 H, CH_2CH_3), 1.01 (t, J = 7.34 Hz, 6 H, CH_2CH_3) ppm. ^{13}C NMR ($CDCl_3$, 125 MHz): δ = 167.74, 157.73, 155.88, 145.65, 138.54, 134.51, 129.10, 124.04, 119.69, 109.17, 52.04, 48.73, 29.69, 21.61, 16.74, 14.00 ppm. IR (KBr pellet): $\tilde{\nu}$ = 3446, 2962, 2361, 1703, 1596, 1436, 1340, 1272, 1262, 1206, 1175, 1065, 1002, 882, 769 cm^{-1}.

Synthesis of H_2L_1: A solution of A_2 (0.151 g, 0.255 mmol) in methanol (5.0 mL)/10% aqueous sodium hydroxide (5.0 mL) was heated to reflux for 3 h. The methanol was then removed under reduced pressure. To the reaction mixture was added water (3 mL), and the pH was adjusted to 6 by the addition of glacial AcOH. This resulted in a white precipitate. The H_2L_1 was recovered by filtration. Yield: 0.111 g, 85.22%. M.p. >300 °C. $C_{27}H_{25}N_5O_4$ (483.52): calcd. C 67.07, H 5.21, N 14.48; found C 67.30, H 5.02, N 14.23. ^{1}H NMR (500 MHz, [D$_6$]DMSO): δ = 7.85 (s, 2 H, Ar-H), 7.79 (t, J = 7.64 Hz, 1 H, pyridine-H), 7.59 (s, 2 H, Ar-H), 7.23 (d, J = 7.64 Hz, 2 H, pyridine-H), 5.50 (s, 4 H, pyridine-CH_2), 2.65 (s, 6 H, N=CCH_3), 2.38 (s, 6 H, Ar-CH_3) ppm. ^{13}C NMR ([D$_6$]DMSO, 125 MHz): δ = 168.74, 156.26, 155.11, 145.25, 138.87, 134.81, 127.78, 124.66, 123.47, 121.17, 109.86, 48.44, 16.75, 14.01 ppm. IR (KBr pellet): $\tilde{\nu}$ = 3442, 2924, 2854, 1683, 1589, 1576, 1455, 1423, 1383, 1347, 1271, 1239, 1199, 1039, 995, 788, 772 cm^{-1}. UV/Vis (MeOH): λ_{max} (ε) = 270 (3.03×10^4 M^{-1} cm^{-1}) nm.

Synthesis of H_2L_2: A solution of B_2 (0.365 g, 0.64 mmol) in methanol (10.0 mL)/10% aqueous sodium hydroxide (10.0 mL) was heated to reflux for 3 h. The methanol was removed under reduced pressure. To the reaction mixture was added water (6 mL), and the pH was adjusted to 6 by the addition of glacial AcOH to give a white precipitate. The H_2L_2 was obtained by filtration. Yield: 0.310 g, 89.46%. M.p. >300 °C. $C_{31}H_{33}N_5O_4$ (539.62): calcd. C 69.00, H 6.16, N 12.98; found C 68.91, H 6.19, N 12.72. ^{1}H NMR (500 MHz, [D$_6$]DMSO): δ = 7.82 (s, 2 H, Ar-H), 7.80 (t, J = 7.7 Hz, 1 H, pyridine-H), 7.59 (s, 2 H, Ar-H), 7.23 (d, J = 7.7 Hz, 2 H, pyridine-H), 5.49 (s, 4 H, pyridine-CH_2), 2.56 (s, 6 H, Ar-CH_3), 2.52 (t, J = 7.76 Hz, 4 H, N=CCH_2), 1.56 (m, 4 H, CH_2CH_3), 0.76 (t, J = 7.3 Hz, 6 H, CH_2CH_3) ppm. ^{13}C NMR ([D$_6$]DMSO, 125 MHz): δ = 168.45, 158.27, 156.30, 145.57, 138.68, 134.86, 127.98, 123.31, 121.12, 109.93, 48.08, 29.06, 16.84, 14.16 ppm. IR (KBr pellet): $\tilde{\nu}$ = 3438, 2964, 2931, 2870, 1676, 1619, 1597, 1505, 1424, 1343, 1277, 1210, 1095, 890, 777 cm^{-1}. UV/Vis (MeOH): λ_{max} (ε) = 275 (5.37×10^4 M^{-1} cm^{-1}) nm.

Synthesis of $[\{Mn_2(L_1)_2(H_2O)_2\}\cdot 2CH_3OH]_n$ (1): To a CH_3OH solution (9 mL) of H_2L_1 (0.026 g, 0.05 mmol) was added 0.1 M aqueous NaOH to adjust the pH = 7. An aqueous solution (3 mL) of $Mn(AcO)_2\cdot 4H_2O$ (0.012 g, 0.05 mmol) was then added dropwise with continuous stirring. The reaction mixture was filtered and left to stand at room temperature. On slow evaporation of the solution over several days, light yellow crystals of **1** suitable for X-ray analysis formed. $C_{56}H_{58}Mn_2N_{10}O_{12}$ (1173.01): calcd. C 57.34, H 4.98, N 11.94; found C 57.42, H 4.89, N 11.85. IR (KBr pellet): $\tilde{\nu}$ = 3451, 2925, 1575, 1549, 1537, 1488, 1418, 1395, 1374, 1346, 1331, 1270, 1222, 1093, 1026, 792 cm^{-1}. UV/Vis (MeOH): λ_{max} (ε) = 270 (4.07×10^3 M^{-1} cm^{-1}) nm.

Synthesis of $[\{Mn_2(L_2)_2(CH_3OH)_4\}\cdot 2CH_3OH\cdot 4H_2O]_n$ (2): To a CH_3OH solution (8 mL) of H_2L_2 (0.054 g, 0.1 mmol) was added 0.1 M aqueous NaOH to adjust the pH to 7. A CH_3OH/H_2O (2:1) solution (6 mL) of $Mn(AcO)_2\cdot 4H_2O$ (0.024 g, 0.1 mmol) was then added dropwise with continuous stirring. The reaction mixture was filtered and left to stand at room temperature. On slow evaporation of the solution over several days, light yellow crystals of **2** suitable for X-ray analysis formed. $C_{68}H_{94}Mn_2N_{10}O_{18}$ (1457.91): calcd. C 56.35, H 6.54, N 9.66; found C 56.23, H 6.69, N 9.57. IR (KBr pellet): $\tilde{\nu}$ = 3405, 2967, 1615, 1576, 1542, 1489, 1416, 1399, 1371, 1337, 1219, 1092, 791 cm^{-1}. UV/Vis (MeOH): λ_{max} (ε) = 270 (8.62×10^3 M^{-1} cm^{-1}) nm.

Table 3. Crystal data and structure refinement details for **1** and **2**.

	1	**2**
Empirical formula	$C_{56}H_{58}Mn_2N_{10}O_{12}$	$C_{68}H_{94}Mn_2N_{10}O_{18}$
Formula mass	1173.01	1449.41
Temperature [K]	273(2)	294(2)
Wavelength [Å]	0.71073	0.71073
Crystal system	triclinic	triclinic
Space group	$P\bar{1}$	$P\bar{1}$
a [Å]	11.1175(9)	9.4384(18)
b [Å]	11.5437(10)	13.276(2)
c [Å]	11.6647(10)	15.471(3)
α [°]	85.729(6)	108.623(3)
β [°]	89.691(6)	101.658(3)
γ [°]	61.458(6)	91.449(3)
V [Å^3]	1310.65(19)	1790.7(6)
Z, calcd. density [Mg m^{-3}]	1, 1.486	1, 1.344
Absorption coefficient [mm^{-1}]	0.557	0.428
F(000)	610	766
Crystal size [mm]	$0.24 \times 0.22 \times 0.20$	$0.22 \times 0.18 \times 0.16$
θ range for data collection [°]	2.09–28.33	1.42–25.02
Limiting indices	$-14 \le h \le 14$, $-15 \le k \le 15$, $-15 \le l \le 14$	$-11 \le h \le 10$, $-15 \le k \le 10$, $-16 \le l \le 18$
Reflections collected/unique	22569/6447 (R_{int} = 0.0603)	9114/6274 (R_{int} = 0.0300)
Refinement method	full-matrix least-squares on F^2	full-matrix least-squares on F^2
Data/restraints/parameters	6447/0/365	6274/121/463
Goodness of fit on F^2	1.015	1.011
Final R indices [$I > 2\sigma(I)$]	R_1 = 0.0616, wR_2 = 0.1587	R_1 = 0.0677, wR_2 = 0.1652
R indices (all data)	R_1 = 0.0970, wR_2 = 0.1790	R_1 = 0.1269, wR_2 = 0.2075

 © 2008 Wiley-VCH Verlag GmbH & Co. KGaA, Weinheim

X-ray Crystallographic Study: Crystals with dimensions $0.24 \times 0.22 \times 0.20$ mm for **1** and $0.22 \times 0.18 \times 0.16$ mm for **2** were selected for X-ray diffraction experiments. The measurements were performed with a Bruker SMART 1000 CCD diffractometer at room temperature (293 K) with graphite-monochromated Mo-K_α radiation (λ = 0.71073 Å). Semi-empirical absorption corrections were applied by using the SADABS program. The structures were solved by direct methods and refined by full-matrix least-squares on F^2 using the SHELXS-97 and SHELXL-97 programs.[29] All non-hydrogen atoms were refined with anisotropic displacement parameters, and the hydrogen atoms were generated geometrically and treated by a mixture of independent and constrained refinements. A summary of the crystallographic data and details of the structure refinements are listed in Table 3. CCDC-662983 (**1**) and -629000 (**2**) contain the supplementary crystallographic data for this paper. These data can be obtained free of charge from The Cambridge Crystallographic Data Centre via www.ccdc.cam.ac.uk/data_request/cif.

Acknowledgments

This work is supported by the National Natural Science Foundations of China (No. 20671014 and 20671012), the Youth Foundation of Beijing Normal University (No. 10770005) and the Key Laboratory of Radiopharmaceuticals of Beijing Normal University, Ministry of Education.

[1] a) *Magnetism: Molecules to Materials* (Eds.: J. S. Miller, M. Drillon), Wiley-VCH, Weinheim, **2002**, vol. 3; b) H. O. Stumpf, L. Ouahab, Y. Pei, D. Grandjean, O. Kahn, *Science* **1993**, *261*, 447–449; c) S. Konar, P. S. Mukherjee, E. Zangrando, F. Lloret, R. N. Chaudhuri, *Angew. Chem. Int. Ed.* **2002**, *41*, 1561–1563; d) H. Miyasaka, N. Matsumoto, H. Okawa, N. Re, E. Gallo, C. Floriani, *J. Am. Chem. Soc.* **1996**, *118*, 981–994; e) E. W. Lee, Y. Kim, D.-Y. Jung, *Inorg. Chem.* **2002**, *41*, 501–506; f) J. Kim, J. M. Lim, Y. K. Choi, Y. K. Do, *Angew. Chem. Int. Ed. Engl.* **1996**, *35*, 998–1000; g) N. Guillou, S. Pastre, C. Livage, G. Ferey, *Chem. Commun.* **2002**, 2358–2359.

[2] a) C. T. Chen, K. S. Suslick, *Coord. Chem. Rev.* **1993**, *128*, 293–322; b) S. D. Cox, T. E. Gier, G. D. Stucky, J. Bierlein, *J. Am. Chem. Soc.* **1988**, *110*, 2986–2987; c) M. Monfort, I. Resino, J. Ribas, X. Solans, M. Font-Bardia, P. Rabu, M. Drillon, *Inorg. Chem.* **2000**, *39*, 2572–2576; d) G. S. Matouzenko, G. Molnar, N. Brefuel, M. Perrin, A. Bousseksou, S. A. Borshch, *Chem. Mater.* **2003**, *15*, 550–556; e) *Extended Linear Chain Compounds* (Ed.: J. S. Miller), Plenum, New York, **1982**, vol. 3.

[3] a) K. Barthelet, J. Marrot, D. Riou, G. Ferey, *Angew. Chem. Int. Ed.* **2002**, *41*, 281–284; b) E. Q. Gao, S. Q. Bai, Z. M. Wang, C. H. Yan, *J. Am. Chem. Soc.* **2003**, *125*, 4984–4985; c) M. Minguet, D. Luneau, E. Lhotel, V. Villar, C. Paulsen, D. B. Amabilino, J. Veciana, *Angew. Chem. Int. Ed.* **2002**, *41*, 586–589; d) B. O. Patrick, W. M. Reiff, V. Sanchez, A. Storr, R. C. Thompson, *Inorg. Chem.* **2004**, *43*, 2330–2339; e) J. R. Galan-Mascaros, K. R. Dunbar, *Angew. Chem. Int. Ed.* **2003**, *42*, 2289–2293; f) H. L. Sun, B. Q. Ma, S. Gao, G. Su, *Chem. Commun.* **2001**, 2586–2587; g) K. Okada, O. Nagao, H. Mori, M. Kozaki, D. Shiomi, K. Sato, T. Takui, Y. Kitagawa, K. Yamaguchi, *Inorg. Chem.* **2003**, *42*, 3221–3228.

[4] a) E. Colacio, J. M. Domínguez-Vera, M. Ghazi, R. Kivekäs, M. Klinga, J. M. Moreno, *Eur. J. Inorg. Chem.* **1999**, 441–445 and references cited therein; b) P. King, R. Clerac, C. E. Anson, C. Coulon, A. K. Powell, *Inorg. Chem.* **2003**, *42*, 3492–3500; c) D. Schulz, T. Weyhermüller, K. Wieghardt, C. Butzlaff, A. X. Trautwein, *Inorg. Chim. Acta* **1996**, *246*, 387–394.

[5] a) J. D. Martin, R. F. Hess, *Chem. Commun.* **1996**, 2419–2420; b) W. Chen, Q. Yue, C. Chen, H. M. Yuan, W. Xu, J. S. Chen, S. N. Wang, *Dalton Trans.* **2003**, 28–30; c) H. H. Zhao, C. P. Berlinguette, J. Bacsa, A. V. Prosvirin, J. K. Bera, S. E. Tichy, E. J. Schelter, K. R. Dunbar, *Inorg. Chem.* **2004**, *43*, 1359–1369.

[6] a) N. A. Law, M. T. Caudle, V. L. Pecoraro, *Adv. Inorg. Chem.* **1999**, *46*, 305–440; b) R. L. Rardin, P. Poganiuch, A. Bino, D. P. Goldberg, W. B. Tolman, S. C. Liu, S. J. Lippard, *J. Am. Chem. Soc.* **1992**, *114*, 5240–5249; c) K. F. Hsu, S. L. Wang, *Inorg. Chem.* **2000**, *39*, 1773–1778.

[7] a) O. M. Yaghi, M. O'Keeffe, N. W. Ockwig, H. K. Chae, J. Kim, M. Eddaoudi, *Nature* **2003**, *423*, 705–714; b) S. L. James, *Chem. Soc. Rev.* **2003**, *32*, 276–288; c) C. Janiak, *Dalton Trans.* **2003**, 2781–2804; d) J. S. Seo, D. Whang, H. Lee, S. Jun, J. Oh, Y. J. Jeon, K. Kim, *Nature* **2000**, *404*, 982–986; e) G. J. Halder, C. J. Kepert, B. Moubaraki, K. S. Murray, J. D. Cashion, *Science* **2002**, *298*, 1762–1765; f) T. Kusukawa, M. Fujita, *J. Am. Chem. Soc.* **2002**, *124*, 13576–13582.

[8] a) M. Fujita, N. Fujita, K. Ogura, K. Yamaguchi, *Nature* **1999**, *400*, 52–55; b) G. F. Swiegers, T. J. Malefeste, *Chem. Rev.* **2000**, *100*, 3483–3537.

[9] S. R. Seidel, P. J. Stang, *Acc. Chem. Res.* **2002**, *35*, 972–983.

[10] a) D. A. Beauchamp, S. J. Loeb, *Chem. Commun.* **2002**, 2484–2485; b) M. Fujita, K. Umemoto, M. Yoshizawa, N. Fujita, T. Kusukawa, K. Biradha, *Chem. Commun.* **2001**, 509–518.

[11] C. Janiak, *J. Chem. Soc., Dalton Trans.* **2000**, 3885–3896.

[12] a) C.-Y. Su, Y.-P. Cai, C.-L. Chen, H.-X. Zhang, B.-S. Kang, *J. Chem. Soc., Dalton Trans.* **2001**, 359–361; b) C.-Y. Su, Y.-P. Cai, C.-L. Chen, F. Lissner, B.-S. Kang, W. Kaim, *Angew. Chem. Int. Ed.* **2002**, *41*, 3371–3375.

[13] C.-Y. Su, Y.-P. Cai, C.-L. Chen, M. D. Smith, W. Kaim, H.-C. zur Loye, *J. Am. Chem. Soc.* **2003**, *125*, 8595–8613.

[14] a) B. Morzyk-Ociepa, D. Michalska, A. Pietraszko, *J. Mol. Struct.* **2004**, *688*, 79–86; b) B. Morzyk-Ociepa, D. Michalska, A. Pietraszko, *J. Mol. Struct.* **2004**, *688*, 87–94.

[15] K. Nakamoto, *Infrared and Raman Spectra of Inorganic and Coordination Compounds*, John Wiley & Sons, New York, **1986**.

[16] C. B. Ma, C. N. Chen, Q. T. Liu, F. Chen, D. Z. Liao, L. C. Li, L. C. Sun, *Eur. J. Inorg. Chem.* **2004**, *16*, 3316–3325.

[17] S. W. Jin, W. Z. Chen, H. Y. Qiu, *Cryst. Growth Des.* **2007**, *7*, 2071–2079.

[18] a) L. Raehm, L. Mimassi, C. Guyard-Duhayon, H. Amouri, *Inorg. Chem.* **2003**, *42*, 5654–5659; b) L. Mimassi, C. Guyard-Duhayon, L. Raehm, H. Amouri, *Eur. J. Inorg. Chem.* **2002**, 2453–2457; c) M. J. Plater, M. R. St. J. Foreman, E. Coronado, C. J. Gómez-García, A. M. Z. Slawin, *J. Chem. Soc., Dalton Trans.* **1999**, *23*, 4209–4216.

[19] a) D. Armentano, G. de Munno, F. Guerra, J. Faus, F. Lloret, M. Julve, *Dalton Trans.* **2003**, 4626–4634; b) D.-G. Huang, X.-F. Zhang, C.-N. Chen, F. Chen, Q.-T. Liu, D.-Z. Liao, L.-C. Li, L.-C. Sun, *Inorg. Chim. Acta* **2003**, *353*, 284–291.

[20] a) C. J. Milios, E. Kefalloniti, C. P. Raptopoulou, A. Terzis, A. Escuer, R. Vicente, S. P. Perlepes, *Polyhedron* **2004**, *23*, 83–95 (and references cited therein); b) R. Cortes, M. Drillon, X. Solans, L. Lezama, T. Rojo, *Inorg. Chem.* **1997**, *36*, 677–683; c) V. Tangoulis, G. Psomas, C. Dendrinou-Samara, C. P. Raptopoulou, A. Terzis, D. Kessissoglou, *Inorg. Chem.* **1996**, *35*, 7655–7660; d) H. Iikura, T. Nagata, *Inorg. Chem.* **1998**, *37*, 4702–4711 (and references cited therein).

[21] T. K. Maji, S. Sain, G. Mostafa, T. H. Lu, J. Ribas, M. Monfort, N. R. Chaudhuri, *Inorg. Chem.* **2003**, *42*, 709–716.

[22] X. S. Tan, D. F. Xiang, W. X. Tang, J. Sun, *Polyhedron* **1997**, *16*, 689–694.

[23] E. Colacio, J.-P. Costes, R. Kivekas, J.-P. Laurent, J. Ruiz, *Inorg. Chem.* **1990**, *29*, 4240–4246.

[24] C. Ruiz-Perez, M. Hernandez-Molina, P. Lorenzo-Luis, F. Lloret, J. Cano, M. Julve, *Inorg. Chem.* **2000**, *39*, 3845–3852.

[25] R. H. Wang, D. Q. Yuan, F. L. Jiang, L. Han, S. Gao, M. C. Hong, *Eur. J. Inorg. Chem.* **2006**, 1649–1656.

 © 2008 Wiley-VCH Verlag GmbH & Co. KGaA, Weinheim

[26] E. Ruiz, S. Alvarez, P. Alemany, *Chem. Commun.* **1998**, 2767–2768.
[27] L.-C. Yang, C.-M. Qi, G.-X. Zhang, N.-Z. Zou, *J. Heterocycl. Chem.* **2003**, *40*, 1107–1112.
[28] M. E. Haeg, B. J. Whitlock, H. W. Whitlock Jr, *J. Am. Chem. Soc.* **1989**, *111*, 692–696.
[29] G. M. Sheldrick, *SHELXS-97 and SHELEXL-97, Programs for the Solution and Refinement of Crystal Structures*, University of Göttingen, Göttingen, Germany, **1997**.

Received: April 11, 2008
Published Online: July 23, 2008

 © 2008 Wiley-VCH Verlag GmbH & Co. KGaA, Weinheim